ECLÉTICA Química

Volume 28 (2003) número 1

Editora UNESP

www.scielo.br/eq

STRUCTURAL BIOINFORMATICS STUDY OF CYCLIN-DEPENDENT KINASES COMPLEXED WITH INHIBITORS

F. CANDURI[1]; N. J. F. da SILVEIRA[1]; J. C. CAMERA JR[1]; W. F. de AZEVEDO JR [2]

Abstract

The present work describes molecular models for the binary complexes CDK9, CDK5 and CDK1 complexed with Flavopiridol and Roscovitine. These structural models indicate that the inhibitors strongly bind to the ATP-binding pocket of CDKs and the structural comparison with the complexes CDK2:Flavopiridol and CDK2:Roscovitine correlates the structural differences with differences in inhibition of these CDKs by the inhibitors. These structures open the possibility of testing new inhibitor families, in addition to new substituents for the already known lead structures such as flavones and adenine derivatives.

Keywords: CDK, Flavopiridol, bioinformatics, structure, drug design.

Introduction

Cell cycle progression is tightly controlled by the activity of cyclin-dependent kinases (CDKs) [31]. CDKs are inactive as monomers, and activation requires binding to cyclins, a diverse family of proteins whose levels oscillate during the cell cycle, and phosphorylation by CDK-activating kinase (CAK) on a specific threonine residue [19]. In addition to the positive regulatory role of cyclins and CAK, many negative regulatory proteins (CDK inhibitors, CKIs) have been discovered [34]. Since deregulation of cyclins and/or alteration or absence of CKIs have been associated with many cancers, there is strong interest in CDKs inhibitors that could play an important role in the discovery of a new family of antitumor agents [17]. CDKs also play a role in apoptosis (CDK2), in neuronal cells (CDK5) and in the control of transcription (CDK7, 8, 9) [9,20].

CDK5 is unique in the sense that although it is widely expressed in many tissues and cells, the CDK5 kinase activity is restricted to neuronal cells [10]. This specificity for neuronal tissue is the result of the CDK5 activator proteins p35, p25, and p39. CDK5 is a multifunctional kinase that associates with other cell proteins to interact with the cytoskeleton and form supramolecular complexes. Recent investigations have revealed that most of the CDK5 in cells forms large multimeric complexes of high molecular weight, ranging from 60 to 670 kDa, in which it is associated with p25, p35,

[1]Departamento de Física - IBILCE, UNESP – CEP 15054-000 – São José do Rio Preto - SP- Brasil.
[2]Center for Applied Toxinology .- Instituto Butantan – CEP 05503-900 - São Paulo – SP -. Brasil.

synapsin, tau, b-catenins, and N-cadherins [33]. Increased CDK5 kinase activity has been implicated in Alzheimer´s disease. Furthermore, pretreatment of cells with CDK5 inhibitors protected them against neuronal death [1]. Since deregulation of CDK5 has been implicated in Alzheimer´s disease, there is strong interest in CDK5 inhibitors that could play an important role in the discovery of anti-Alzheimer´s disease agents.

Flavopiridol a cyclin-dependent kinase (CDK) inhibitor is a potential anti-cancer therapeutic agent currently being tested in phase I and II clinical trials because of its antiproliferative properties. Treatment with Flavopiridol resulted in blocking cell cycle progression, promoting differentiation and inducing apoptosis in various types of cancerous cells [40]. The structure of CDK2 complexed with deschloroflavopiridol revealed that the drug docks in the ATP binding site [17], which helps to explain why inhibition of CDK2 is competitive with ATP.

Two previous studies demonstrated the effect of Flavopiridol on transcription. Mammalian cells treated with this compound showed decreased transcription of the gene encoding cyclin D1 [8], and high levels of Flavopiridol affected levels of 63 different mRNAs in *Saccharomyces cerevisiae* [21]. The transcriptional inhibition observed in these studies could have been direct or a consequence of altered progression through the cell cycle. Furthermore, it has been shown that the binary complex CDK9-Cyclin T1 is potently inhibited by Flavopiridol [9]. These results demonstrated that Flavopiridol inhibited the complex CDK9-Cyclin T1 causing inhibition of transcription. The properties of the Flavopiridol towards the CDK9-Cyclin T1 complex suggest that it should be examined its potential use in HIV-1 therapy [9,14].

Roscovitine is a potent CDK inhibitor and was tested against various CDKs, with IC50 values ranging from 0.16 mM (for CDK5) [15] to over 100 mM (for CDK4 and CDK6) [28].

This article describes the modeling of the human CDK9 complexed with Flavopiridol, CDK5 complexed with Roscovitine, and CDK1 complexed with Roscovitine and Flavopiridol. The investigation was made in order to gain further insight into the structural basis for chemical inhibition of CDKs by Flavopiridol and Roscovitine.

Methods

Molecular modeling

Homology modeling is usually the method of choice when there is a clear relationship of homology between the sequence of a target protein and at least one known structure. This computational technique is based on the assumption that the tertiary structures of two proteins will be similar if their sequences are related, and it is the approach most likely to give accurate results [25]. There are two main approaches to homology modeling: 1) Fragment-based comparative modeling [4, 3] and 2) Restrained-based modeling [36]. For modeling of the CDKs:inhibitor complexes we used the second approach. Model building of CDKs:inhibitor was carried out using the program MODELLER [36]. MODELLER is an implementation of an automated approach to comparative modeling by satisfaction of spatial restraints [37, 38, 35]. The modeling procedure begins with an alignment of the sequence to be modeled (target) with related known three-dimensional structures (templates). This alignment is usually the input to the program. The output is a three-dimensional model for the target sequence containing all mainchain and sidechain non-hydrogen atoms.

Since there is no three-dimensional structure for CDK2:Flavopiridol complex available a model was built based on the atomic coordinates of CDK2:Deschloroflavopridol complex, which was solved by cryocrystallographic methods [17]. The Flavopiridol coordinates, taken from the complex Glycogen Phosphorylase:Flavopiridol (Access code: 1C8K), [32] were superposed to that of CDK2:Deschloroflavopiridol [17] in order to obtain the CDK2:Flavopiridol structure. The atomic coordinates for CDK2:Flavopiridol were used as starting model for modeling of the CDK9 and CDK1 complexed with Flavopiridol. The alignment of CDK2 (template), CDK1, CDK5, and CDK9 is shown in Figure 1. Fifteen residues from the N-terminal and 45 residues from the C-terminus were removed from the CDK9 model, since there is no good template for these fragments, for CDK1 and CDK5 all residues were kept in the model. Next, the spatial restraints and CHARMM energy terms enforcing proper stereochemistry [6] were combined into an objective function. Finally, the model is obtained by optimizing the objective function in Cartesian

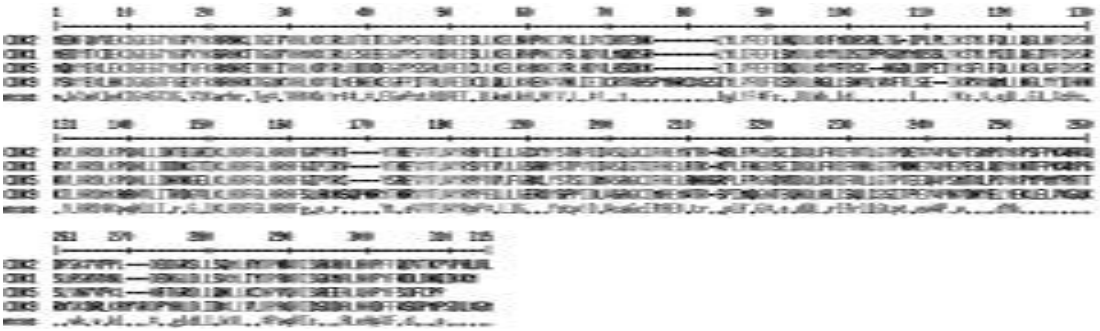

Figure 1: Sequence alignment of human CDK2 with CDK9, CDK1, and CDK5. There are 39.1% of identity between CDK2 and CDK9 sequences, 65.1% between CDK2 and CDK1, and 58.3% between CDK2 and CDK5 sequences. The multiple alignment was performed with the program MultAlin (40).

space. The optimization is carried out by the use of the variable target function method [5] employing methods of conjugate gradients using the program MODELLER [36]. Several slightly different models can be calculated by varying the initial structure. The final model is selected based on stereochemical quality. All optimization process was performed on a Beowulf cluster (16 nodes, AMD Athlon 1800+).

Analysis of the model

The overall stereochemical quality of the final models for CDK9:Flavopiridol, CDK5:Roscovitine, CDK1:Roscovitine, CDK1:Flavopiridol were assessed by the program PROCHECK [26]. Atomic models were superposed using the program LSQKAB from CCP4 [11]. The cutoff for hydrogen bonds and salt bridges was 3.4 Å. The contact surfaces for the binary complexes were calculated using AREAIMOL and RESAREA [11].

Results and Discussion

Quality of the model

Ramachandran diagram f-y plots for the binary complexes of CDK models and for eight crystallographic CDK2 structures solved to resolution better than 2.1 Å were generated (Figures not shown). The Ramachandran plot, for the eight CDK2 structures, was used to compare the overall stereochemical quality of CDKs models against CDK2 structures solved by biocrystallography. Analysis of the Ramachandran plot for the CDK9 model shows that 78.4 % of the residues lie in the most favorable regions and the remaining 21.6 % in the additional allowed regions, the CDK5 model shows that 91.0 % of the residues lie in the most favorable regions, 8.2 % in the additional allowed regions, and 0.8 % in the disallowed regions (Asp 97 and Ala 198), and the CDK1 model shows that 90.8 % of the residues lie in the most favorable regions and 9.2 % in the additional allowed regions. The same analysis for eight crystallographic CDK2 structures present 89.8 % of residues in the most favorable, 9.7 % in additional allowed regions, and 0.5% in generously allowed regions.

Overall description

The models of the kinase in the complexes CDK:inhibitor are folded into the typical bilobal structure, with the smaller N-terminal lobe consisting predominantly of b-sheet structure and the larger C-terminal lobe consisting primarily of α-helices. The N-terminal lobe of CDK consists of a sheet of five antiparallel β-strands (β1-β5) and a single large helix (α1). The C-terminal lobe contains a pseudo-4-helical bundle (α2,3,4,6), a small b-ribbon (β6-β8), and two additional helices (α5,7). Figure 2 shows schematic drawings of the complexes CDK9:Flavopiridol, CDK5:Roscovitine, CDK1:Flavopiridol and CDK1:Roscovitine. The Flavopiridol and Roscovitine molecules are found in the cleft between the two lobes. The core (the β-sheet and the helical bundle) of the CDK9, 5 and 1 structures are very similar to that of CDK2 [18]. The conserved core consists of a small lobe associated primarily with ATP binding and a large lobe associated with peptide binding and catalysis.

In CDK9, the residues 93 to 95 present a β-sheet, while in CDK2 this region (residues 85 to 87) is in random coil. Most of the residues conserved throughout the protein kinase family cluster around the active cleft [41].

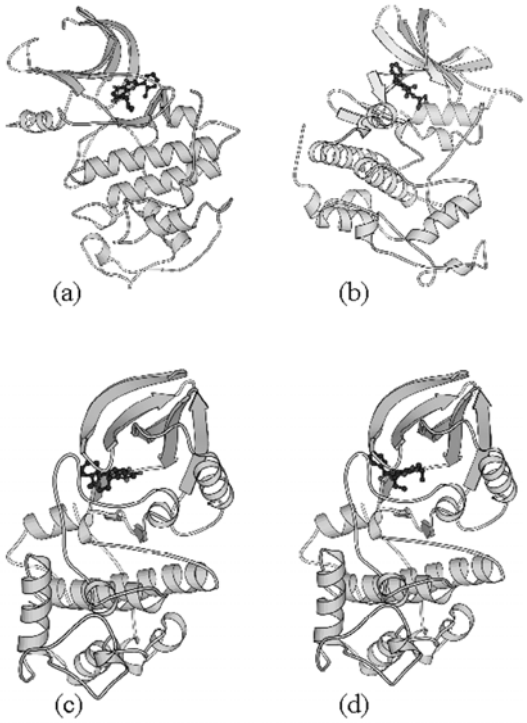

Figure 2: Ribbon diagram of the complex CDK9:Flavopiridol(a),CDK5:Roscovitine(b), CDK1:Flavopiridol (c), and CDK1:Roscovitine (d) generated by Molscript (41).

Molecular fork

It has been observed in several CDK2:inhibitor structures the participation of a molecular fork, composed by a C=O group of Glu81 and the N-H and C=O group of Leu83, in hydrogen bonds between CDK2 and the inhibitor. This molecular fork, composed of two hydrogen bond acceptors (C=O) and one hydrogen bond donor (N-H), allows a wide range of different orientations to dock on to the ATP binding pocket, such as: olomoucine, isopentenyladenine, and roscovitine [39, 16], staurosporine [27], purvalanols [21], indirubins [22], hymenialdisine [29], NU2058 [2]. Table 1 shows the hydrogen bond distances between the molecular fork of CDK2 and different inhibitors. All these inhibitors have pairs of hydrogen bond partners that show complementarity to the molecular fork on CDK2, most of them involving at least two hydrogen bonds with the molecular fork. The relative orientation of the inhibitor in the binding pocket of CDK2 locates one hydrogen bond donor close to C=O in Glu81 and/or Leu83, and an acceptor close to N-H in Leu83. Such simple paradigm is conserved in all CDK2:inhibitor complex structures solved so far. In all binary models this molecular fork is also conserved.

Inhibitor	Distance between inhibitor and C=O on Glu81 (Å)	Distance between inhibitor and N-H on Leu83 (Å)	Distance between inhibitor and C=O on Leu83 (Å)
Staurosporine	2.75	2.63	NO
Purvalanol B	NO	3.18	2.54
Hymenialdisine	2.76	2.74	3.17
NU2058	2.57	3.11	2.34
NU6027	2.84	2.97	2.49
U55	NO	3.30	2.74
PKFO 49-38	2.71	3.13	3.27
Deschloroflavopiridol	2.86	2.91	NO
Roscovitine	NO	3.38	2.82
Olomoucine	NO	2.94	2.65
Isopentenyladenine	NO	3.39	NO
Indirubins	3.04	2.72	3.10

NO: Not observed.

Table 1: Hydrogen bonds between the molecular fork of CDK2 and inhibitor.

Interactions of flavopiridol with CDK9

The specificity and affinity between an enzyme and its inhibitor depend on hydrogen bonds and ionic interactions, as well as on shape complementarity of the contact surfaces of both partners [16, 7, 13]. It was observed a total of three hydrogen bonds between CDK9 and Flavopiridol, in binary model, involving the residues Lys 33, Asp 89, Cys 91. For the CDK2:Flavopiridol model four hydrogen bonds involving the residues Lys33, Glu81, Leu83, and Asp152 were observed. Table 2 and 3 show the intermolecular hydrogen bonds for both structures. As observed for the crystallographic structure of deschloroflavopiridol bound to CDK2 [17], the region of CDK9 occupied by the chlorophenyl ring of Flavopiridol is pointing away from the ATP-binding pocket, and partially exposed to solvent.

Hydrogen bonds between active site and inhibitor			Distance (Å)
Flavopiridol	CDK9		
O3	Lys33	NZ	3.40
O5	Asp89	O	2.77
O4	Cys91	N	2.75

Table 2: Hydrogen bonds between CDK9: Flavopiridol.

Hydrogen bonds between active site and inhibitor			Distance (Å)
Flavopiridol	CDK2		
O5	Glu81	O	2.88
O4	Leu83	N	2.73
O3	Asp152	OD2	3.19
O3	Lys33	NZ	3.03

Table 3: Hydrogen bonds between CDK2: Flavopiridol.

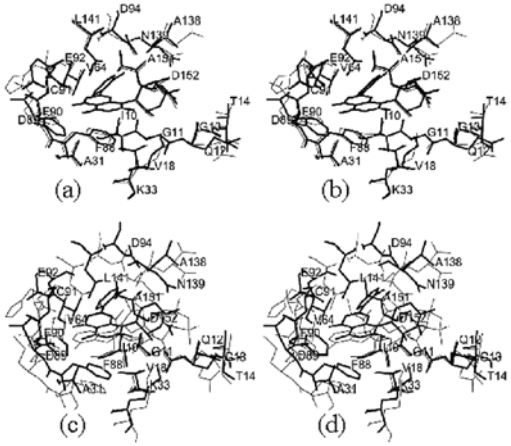

Figure 3: (a) Superimposed binding pockets of CDK9:Flavopiridol complex (thick line) and CDK2:Flavopiridol complex (thin line). (Rmsd value for C : 0.169Å) (b) Superimposed binding pockets of CDK9:Flavopiridol complex (thick line) and CDK2:ATP complex (thin line). (Rmsd value for C : 0.465Å).

Superposition of the complexes of Flavopiridol with CDK2 and CDK9 is shown in Figure 3a. The benzopyran ring of Flavopiridol occupies the same region in both complexes. This region is the same occupied by the purine ring of ATP in the CDK2:ATP complex [23]. Superposition of the CDK2:ATP onto CDK9:Flavopiridol structure indicates that the two ring systems overlap approximately in the same plane. Figure 3b shows the ATP-binding pocket for the complexes CDK2:ATP and CDK9:Flavopiridol.

The CDK structures are constituted of two lobes and two strong salt bridges are observed involving Glu 92 - Lys 20 and Glu 92 - Lys 29 in the CDK9:Flavopiridol structure. These salt bridges involve residues from two lobes of the CDK9 structure and they are not conserved in the CDK2 structures. Lys 20 and 29 in the N-terminal lobe and Glu 92 in the C-terminal lobe of CDK2 do not form salt bridges. This strong electrostatic interaction brings the two lobes of CDK9 closer, which increases the enzyme-inhibitor contact area, however CDK9 makes only three hydrogen bonds with flavopiridol. Figure 4: shows the position of the salt bridges in the CDK9 structure. Furthermore, the side chains of Glu 92, Lys 20 and Lys 29 bring the phenyl of Phe 90 to a position deeper in the binding pocket, which also contributes to increase the contact area between Flavopiridol and CDK9.

Figure 4: Ribbon diagram of the human CDK9 generated by Molscript (35) showing the residues Lys 20, Lys 29, Phe 90 and Glu 92.

Chao *et al.*, (2000) performed a functional study of inhibition of CDK9 by Flavopiridol, which indicated lack of competition with ATP, suggesting the presence of at least one additional binding site [9]. However a close inspection of the structure of the CDK9 model did not reveal the presence of any additional binding pockets. The CDK9:Flavopiridol model clearly reveals a very tight binding of the inhibitor to the enzyme which may essentially inactivate the enzyme, in such scenery a competitive kinetic mechanism is possible.

The contact areas for the complexes of CDK2 and CDK9 with Flavopiridol are 320 Å^2 and 332 Å^2 respectively, which may partially explain the lower IC50 value observed for CDK9. Table 4 summarizes the some structural results and IC50 for CDK2 and CDK9 structures. The overall structure of the complex indicates that the Flavopiridol is tightly bound to the ATP-binding pocket and since no further binding sites were identified in the CDK9 structure we have strong structural evidence that Flavopiridol is a competitive inhibitor with ATP.

	CDK2	CDK9
Contact area for the complexes with flavopiridol (Å^2)	320	332
Number of Hydrogen bonds between protein and inhibitor	5	6
IC50 (μM)	0.4	0.2

Table 4: Summary of structural results for CDK2 and CDK9.

The simple paradigm of the molecular fork, also identified in the CDK9 structure, suggests that CDK9 may also be strongly inhibited by other CDK2 inhibitors, such as roscovitine, olomoucine, and staurosporine. Further inhibition experiments may confirm this prediction. Figure 5 shows a schematic diagram for this molecular fork.

It has been observed that the complex CDK9-Cyclin T1 is a key factor in HIV-1 infection and Flavopiridol blocks HIV-1 propagation in cultured cells. Furthermore, it has been suggested that Flavopiridol should be evaluated in AIDS therapy [9] so that the CDK9 structural model can be used for designing new active CDK9 inhibitors.

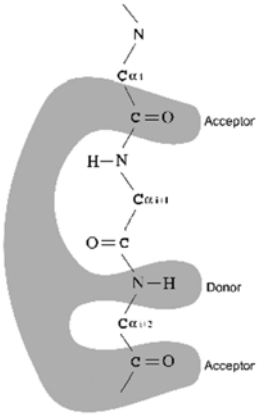

Figure 5: Schematic diagram of the molecular fork. Residues from i to i+2 are Glu81, Phe82, Leu83 and Asp89, Phe90, Cys91 for CDK2 and CDK9, respectively.

Interactions of Roscovitine with CDK5

It was observed a total three hydrogen bonds between CDK5 and Roscovitine, in binary model, involving the residues Cys83, Asp86, and Gln130. For the CDK2:Roscovitine model two hydrogen bonds involving the residue Leu83 were observed. Table 5 shows the intermolecular hydrogen bonds for both complexes. The higher number of intermolecular hydrogen bonds, observed in the CDK5:Roscovitine complex, is probably due to the modification of His84 (CDK2) to Asp in the CDK5 sequence, which allows an additional salt-bridge in the CDK5 structure, involving Asp84 and Lys20. This salt-bridge moves the inhibitor away from the molecular fork of CDK5, however keeping the intermolecular hydrogen bonds between the molecular fork and Roscovitine. Nevertheless, this movement brings Roscovitine closer to the side chains of Gln130 and Asp86, allowing additional intermolecular hydrogen bonds.

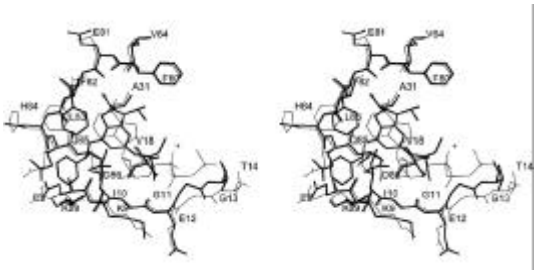

Figure 6: Superimposed binding pockets of CDK5:Roscovitine complex (thick line) and CDK2:ATP complex (thin line) (Rmsd value for Cα: 0.576Å)

Roscovitine.

Roscovitine	CDK	Residue, atom	Distance (Å)
N6	CDK2	Leu 83 O	2.82
N7	CDK2	Leu 83 N	3.38
N6	CDK5	Cys83 O	3.10
O1	CDK5	Gln 130 NE2	3.29
N1	CDK5	Asp86 OD2	3.16

Table 5: Intermolecular hydrogen bonds between CDK2 and Roscovitine, and CDK5 and Roscovitine.

Superposition of the CDK2:ATP onto CDK5: Roscovitine structure indicates that the two ring systems of Roscovitine and ATP overlap approximately in the same plane, however with different orientations. As observed for the crystallographic structure of the CDK2:Roscovitine complex [16] the region of CDK5 occupied by the phe-

nyl ring of Roscovitine is pointing away from the ATP-binding pocket, and partially exposed to solvent. Figure 6 shows the ATP-binding pocket for the complexes CDK2:ATP and CDK5:Roscovitine.

Interactions of Flavopiridol and Roscovitine with CDK1

A total of five hydrogen bonds between CDK1 and Flavopiridol, involving the residues Lys33, Glu81, Leu83, and Asp146 were observed for the binary complex. Table 6 shows the intermolecular hydrogen bonds for structure of Flavopiridol complexed with CDK1. It was observed a total of four hydrogen bonds between CDK1 and Roscovitine, in the binary model, involving the residues Leu83, Asp86, and Gln132. For the CDK2:Roscovitine model only two hydrogen bonds, involving the residue Leu83, were observed. Table 7 shows the intermolecular hydrogen bonds for CDK1: Roscovitine complex. As observed in the crystallographic structure of CDK2:Roscovitine [16], and for the CDK2: Flavopiridol model [17] the region of CDK1 occupied by the phenyl ring of Roscovitine and the chlorophenyl of Flavopiridol is pointing away from the ATP-binding pocket, and partially exposed to solvent in both complexes.

Hydrogen bonds between active site and inhibito			Distance (Å)
Flavopiridol	CDK1		
O5	Glu81	O	2.65
O4	Leu83	N	2.81
O7	Asp146	OD2	3.23
O7	Lys33	NZ	2.97
O3	Lys33	NZ	3.27

Table 6: Intermolecular hydrogen bonds between CDK1 and Flavopiridol.

Hydrogen bonds between active site and inhibito			Distance (Å)
Roscovitine	CDK1		
N6	Leu83	O	3.36
O1	Gln132	NE2	3.38
N1	Asp86	OD2	3.16
N2	Asp86	OD2	3.30

Table 7: Intermolecular hydrogen bonds between CDK1 and Roscovitine.

Conclusions

The overall structure of all complexes indicates that Roscovitine and Flavopiridol are tightly bound to the ATP-binding pocket, and no further binding sites were identified in the CDK structures.

The analysis of the structural models and activity experiments strongly indicates that the comparison of structures of different enzymes complexed with same inhibitor (Roscovitine complexed with CDK1 and CDK2, and Flavopiridol complexed with CDK1 and CDK2) can be used for a qualitative analysis of the activity of these inhibitors against different enzymes. Furthermore, the molecular fork identified in CDK2 structures seems to be conserved in the CDK1, CDK5 and CDK9 models, and being also involved in hydrogen bonds with the inhibitors, this suggests that CDK1, 5, and 9 may also be strongly inhibited by other CDK2 inhibitors. Further inhibition experiments may confirm this prediction.

Acknowledgments

This work was supported by grants from FAPESP (SMOLBNet – Proc. n. 01/07532-0), CNPq, and CAPES. WFAJr. is a researcher for the Brazilian Council for Scientific and Technological Development (CNPq, 300851/98-7).

CANDURI, F.; SILVEIRA, N. J. F. da; CAMERA JR, J. C.; AZEVEDO JR, W. F. de.Estudo de bioinformática estrutural de quinases dependentes de ciclinas complexadas com inibidores.

Resumo

O presente trabalho descreve modelos moleculares para os complexos binários CDK9, CDK5 e CDK1 complexados com Flavopiridol e Roscovitina. Esses modelos estruturais indicam que os inibidores ligam-se fortemente ao sítio de ligação de ATP das CDKs e comparações estruturais dos complexos CDK2-Flavopiridol e CDK2-Roscovitina relacionam diferenças estruturais com diferenças na inibição dessas CDKs por esses inibidores. Essas estruturas abrem a possibilidade de testar novas famílias de inibidores, em adição aos novos

substituintes para as estruturas já conhecidas, tais como flavonas e derivados de adenina.

Palavras-chave: CDK, Flavopiridol, bio-informática, estrutura, desenho de drogas.

References

[1] ALVAREZ, A.; TORO, R.; CÁCERES, A.; MACCIONI, R. B. Inhibition of tau phosphorylating protein kinase cdk5 prevents beta-amyloid-induced neuronal death. *FEBS Lett*, v. 459, n. 3, p. 421-426, 1999.

[2] ARRIS, C. E.; BOYLE, F. T.; CALVERT, A. H.; CURTIN, N. J.; ENDICOTT, J. A.; GARMAN, E. F.; GIBSON, A. E.; GOLDING, B. T.; GRANT, S.; GRIFFIN, R. J.; JEWSBURY, P.; JOHNSON, L. N.; LAWRIE, A. M.; NEWELL, D. R.; NOBLE, M. E.; SAUSVILLE, E. A.; SCHULTZ, R.; YU, W. Identification of novel purine and pyrimidine cyclin-dependent kinase inhibitors with distinct molecular interactions and tumor cell growth inhibition profiles. *J. Med. Chem*., v. 43, n. 15, p. 2797-2804, 2000.

[3] BLUNDELL, T. L.; CARNEY, D.; GARDNER, S.; HAYES, F.; HOWLIN, B.; HUBBARD, T.; OVERINGTON, J.; SINGH, D. A.; SIBANDA, B. L.; SUTCLIFFE, M. 18th Krebs, Hans lecture – knowledge-based protein modeling and design. *Eur. J. Biochem*., v. 172, n. 3, p. 513-520, 1988.

[4] BLUNDELL, T. L.; SIBANDA, B. L.; STERNBERG, M. J.; THORNTON, J. M. Knowledge-based prediction of protein structures and the design of novel molecules. *Nature*, v. 326, n. 6111, p. 347-352, 1987.

[5] BRAUN, W.; GO, N. Calculation of protein conformations by proton-proton distance constraints. A new efficient algorithm. *J. Mol. Biol*., v. 186, n. 3, p. 611-626, 1985.

[6] BROOKS, B. R.; BRUCCOLERI, R. E.; OLAFSON, B. D.; STATES, D. J.; SWAMINATHAN, S.; KARPLUS, M. CHARMM: a program for macromolecular energy minimization and dynamics calculations. *J. Comp. Chem*., v. 4, p. 187-217, 1983.

[7] CANDURI, F.; TEODORO, L. G. V. L.; LORENZI, C. C. B.; HIAL, V.; GOMES, R. A. S.; RUGGIERO NETO, J.; DE AZEVEDO, W. F. JR. Crystal structure of human uropepsin at 2.45Å resolution. *Acta Crystallogr.,* v. D57, p. 1560-1570, 2001.

[8] CARLSON, B.A.; LAHUSEN, T.; SINGH, S.; LOAIZA-PEREZ, A.; WORLAND, P. J.; PESTELL, R.; ALBANESE, C.; SAUSVILLE, E. A.; SENDEROWICZ, A. M. Downregulation of cyclin D1 by transcriptional repression in MCF-7 human breast carcinoma cells induced by flavopiridol. *Cancer Res*., v. 59, p. 4634-4641, 1999.

[9] CHAO, S. H.; FUJINAGA, K.; MARION, J. E.; TAUBE, R.; SAUSVILLE, E. A.; SENDEROWICZ, A. M.; PETERLIN, B. M; PRICE, D. H. J. Flavopiridol inhibits P-TEFb and blocks HIV-1 replication. *J. Biol. Chem.,* v. 275, n. 37, p. 28345-28348, 2000.

[10] CLARE, P. M.; POORMAN, R. A.; KELLEY, L. C.; WATENPAUGH, K. D.; BANNOW, C. A.; LEACH, K. L. The cyclin-dependent kinases cdk2 and cdk5 act by a random, anticooperative kinetic mechanism. *J. Biol. Chem*., v. 276, p. 48292-48299, 2001.

[11] COLLABORATIVE computational project n. 4. The CCP4 suite: programs for protein crystallography. *Acta Crystallogr.,* v. D50, p. 760-763, 1994.

[12] CORPET, F. Multiple sequence alignment with hierarchical clustering. *Nucl. Acids Res*., v. 16, n. 22, p.10881-10890, 1988.

[13] DE AZEVEDO, W. F. JR.; CANDURI, F.; FADEL, V.; TEODORO, L. G. V. L.; HIAL, V.; GOMES, R. A. S. Molecular model for the binary complex of uropepsin and pepstatin. *Biochem. Biophys. Res. Commun*., v. 287, n. 1, p. 277-281, 2001.

[14] DE AZEVEDO, W. F. JR.; CANDURI, F.; SILVEIRA, N. J. F. Structural basis for inhibition of cyclin-dependent kinase 9 by flavopiridol. *Biochem Biophys. Res. Commun*., v. 293, p. 566-571, 2002.

[15] DE AZEVEDO, W. F. JR.; GASPAR, R. T.; CANDURI, F.; CAMERA, J. C. JR.; SILVEIRA, N. J. F. Molecular model of cyclin-dependent kinase 5 complexed with roscovitine. *Biochem. Biophys. Res. Commun*., v. 297, p. 1154-1158, 2002.

[16] DE AZEVEDO, W. F. JR.; LECLERC, S.; MEIJER, L.; HAVLICEK, L.; STRNAD, M.; KIM, S.-H. Inhibition of cyclin-dependent kinases by purine analogues: crystal structure of human CDK2 complexed with roscovitine. *Eur. J. Biochem*., v. 243, p. 518-526, 1997.

[17] DE AZEVEDO, W. F. JR.; MUELLER-DIECKMANN, H.;J.; SCHULZE-GAHMEN, U.; WORLAND, P. J.; SAUSVILLE, E.; KIM S.-H. Structural basis for specificity and potency of a flavonoid inhibitor of human CDK2, a cell cycle kinase. *Proc. Natl. Acad. Sci. USA*., v. 93, n. 7, p. 2735-2740, 1996.

[18] DEBONDT, H. L.; ROSENBLATT, J.; JANCARIK, J.; JONES, H. D.; MORGAN, D. O.; KIM, S.-H. Crystal structural of cyclin-dependent kinase 2. *Nature,* v. 363, p. 595-602, 1993.

[19] DESAI, D.; GU, Y.; MORGAN, D. O. Activation of human cyclin-dependent kinases *in vitro*. *Mol. Biol. Cell,* v. 3, p. 571-582, 1992.

[20] GRAY, N.; DETIVAUD, L.; DOERIG, C.; MEIJER, L. ATP-site directed inhibitors of cyclin-dependent kinases.

Curr. Med. Chem. v. 6, n. 9, p. 859-875, 1999.

[21] GRAY, N. S.; WODICKA, L.; THUNNIESSEN, A. M.; NORMAN, T. C.; KWON, S.; ESPINOZA, F. H.; MORGAN, D. O.; BARNES, G.; LECLERC, S.; MEIJER, L.; KIM, S. H.; LOCKHART, D. J.; SCHULTZ, P. G. Exploiting chemical libraries, structure, and genomics in the search for kinase inhibitors. *Science,* v. 281, p. 533-538, 1998.

[22] HOESSEL, R.; LECLERC, S.; ENDICOTT, J. A.; NOBEL, M. E.; LAWRIE, A.; TUNNAH, P.; LEOST, M.; DAMIENS, E.; MARIE, D.; MARKO, D.; NIEDERBERGER, E.; TANG, W.; EISENBRAND, G.; MEIJER, L. Indirubin, the active constituent of a chinese antileukaemia medicine, inhibits cyclin-dependent kinases. *Nat. Cell Biol.,* v. 1, n. 1, p. 60-67, 1999.

[23] KIM, S.-H.; SCHULZE-GAHMEN, U.; BRANDSEN, J.; DE AZEVEDO, W. F. JR. Structural basis for chemical inhibitor of CDK2. *Prog. Cell Cycle Res.,* v. 2, p. 137-145, 1996.

[24] KRAULIS, P. MOLSCRIPT: a program to produce both detailed and schematic plots of proteins. *J. App. Cryst*., v. 24, p. 946-950, 1991.

[25] KROEMER, R. T.; DOUGHTY, S. W.; ROBINSON, A. J.; RICHARDS, W. G. Prediction of the three-dimensional structure of human interleukin-7 by homology modeling. *Protein Eng.,* v. 9, n. 6, p. 493-498, 1996.

[26] LASKOWSKI, R. A.; MACARTHUR, M. W.; SMITH, D. K.; JONES, D. T.; HUTCHINSON, E. G.; MORRIS, A, L.; NAYLOR, D.; MOSS, D. S.; THORTON, J. M. *PROCHECK v.3.0*: program to check the stereochemistry quality of protein structures - operating instructions, [s.l.:s.n.], 1994.

[27] LAWRIE, A. M.; NOBLE, M. E.; TUNNAH, P.; BROWN, N. R.; JOHNSON, L. N.; ENDICOTT, J. A. Protein kinase inhibition by staurosporine revealed in details of the molecular interaction with CDK2. *Nat. Struct. Biol.,* v. 4, p. 796, 1997.

[28] MEIJER, L.; BORGNE, A.; MULNER, O.; CHONG, J. P.; BLOW, J. J.; INAGAKI, N. Biochemical and cellular effects of roscovitine, a patent and selective inhibitor of the cyclin-dependent kinases CDK2 and CDK5. *Eur. J. Biochem*., v. 243, p. 527-536, 1997.

[29] MEIJER, L.; THUNNISSEN, A. M.; WHITE, A. W.; GARNIER, M.; NIKOLIC, M.; TSAI, L. H.; WALTER, J.; CLEVERLEY, K. E.; SALINAS, P. C.; WU, Y. Z.; BIERNAT, J.; MANDELKOW, E. M.; KIM, S.-H.; PETTIT, G. R. Inhibition of cyclin-dependent kinases, GSK-3beta and CK1 by hymenialdisine, a marine sponge constituent. *Chem. Biol*., v. 7, n. 1, p. 51-63, 2000.

[30] NICHOLLS, A.; SHARP, K. A.; HONIG, B. Protein folding and association: insights from the interfacial and thermodynamic properties of hydrocarbons. *Proteins,* v. 11, n. 4, p. 281-296, 1991.

[31] NORBURY, C.; NURSE, P. Animal cell cycles and their control. *Annu. Rev. Biochem*., v. 61, p. 441-470, 1992.

[32] OIKONOMAKOS, N. G.; SCHNIER, J. B.; ZOGRAPHOS, S. E.; SKAMNAKI, V. T.; TSITSANOU, K. E.; JOHNSON, L. N. Flavopiridol inhibits glycogen phosphorylase by binding at the inhibitor site. *J. Biol. Chem.,* v. 275, n. 44, p. 34566-34573, 2000.

[33] PATRICK, G. N.; ZUKERBERG, L.; NIKOLIC, M.; DE LA MONTE, S.; DIKKES, P.; TSAI, L. H. Conversion of p35 to p25 deregulates Cdk5 activity and promotes neurodegeneration. *Nature*, v. 402, n. 6762, p. 615-22, 1999.

[34] RICHARDSON, H. E.; STUELAND, C. S.; THOMAS, J.; RUSSEL, P.; REED, S. I. Human cDNAs encoding homologs of the small p34Cdc28/Cdc2-associated protein of Saccharomyces cerevisiae and Schizosaccharomyces pombe. *Genes Dev.,* v. 4, p. 1332-1344, 1990.

[35] SALI, A. Modeling mutations and homologous proteins. *Curr. Opin. Biotechnol.,* v. 6, n. 4, p. 437-451, 1995.

[36] SALI, A.; BLUNDELL, T. L. Comparative protein modelling by satisfaction of spatial restraints. *J. Mol. Biol*., v. 234, p. 779-815, 1993.

[37] SALI, A.; OVERINGTON, J. P. Derivation of rules for comparative protein modeling from a database of protein structure alignments. *Protein Sci.*, v. 3, n. 9, p. 1582-1596, 1994.

[38] SALI, A.; POTTERTON, L.; YUAN, F.; VAN VLIJMEN, H.; KARPLUS, M. Evaluation of comparative protein modeling by MODELLER. *Proteins,* v. 23, n. 3, p. 318-326, 1995.

[39] SCHULTZE-GAHMEN, U.; BRANDSEN, J.; JONES, H. D.; MORGAN, D. O.; MEIJER, I.; VESELY, J. Multiple modes of ligand recognition: crystal structures of cyclin-dependent protein kinase 2 in the complex with ATP and two inhibitors, olomoucine and isopentenyladenine. *Proteins,* v. 22, p. 378-391, 1995.

[40] SENDEROWICZ, A. M.; SAUSVILLE, E. A. Preclinical and clinical development of cyclin-dependent kinase modulators. *J. Natl. Cancer Inst.,* v. 92, n. 5, p. 376-387, 2000.

[41] SEROTA, S.; RADSIO-ANDZELM, E. Three protein kinase structures define a common motif. *Structure,* v. 2, p. 345-355, 1994.